SUNGLINT IN AVHRR DATA AND THE DETERMINATION OF NEAR SURFACE WINDSPEEDS

A.P. Cracknell, S. Khattak and R.A. Vaughan
Department of Applied Physics and
Electronic & Manufacturing Engineering,
University of Dundee,
Dundee DD1 4HN, Scotland, U.K.

Abstract: We have developed software to identify automatically those areas on AVHRR data in which sunglint can be expected, by the geometrical and physical conditions, to occur. For a selection of such scenes from 1982-1983, we have used the approach of Cox and Munk to determine near-surface windspeeds and the results have been compared with the very limited surface observations that are available for the areas in question. The results are encouraging.

1.0 INTRODUCTION

This paper describes the software written for the automatic identification of sunglint areas on AVHRR scenes and for the extraction of near-surface windspeeds. The objective was to identify those scenes that contain areas of sunglint, without visual inspection of all the quicklook images, and then to use the data from these scenes to determine the wind velocity utilizing Cox and Munk's model. The spectral channel 2 of the AVHHR data was used for this purpose. This model makes use of the satellite and solar positions and it seems very tedious and time-consuming to find these positions for each relevant point.

The software developed here needs to have available ephemeris data like orbit inclination, equator crossing longitude, equator crossing time and the satellite height.

2.0 SUNGLINT

Sunglint, which is the direct solar reflection from the water surface to the sensor on board the satellite, was reported to be a nuisance in the study of sea surface temperature (Takashima and Takayama 1981 and Burstein 1982) and of ocean colour (Hoge and Swift 1987). On the other hand, sunglint can give useful information to the interpreter about the sea surface roughness, wind velocity, oil slicks and ripples areas. The intensity of the sunglint and the area covered by the sunglint on an AVHRR image depend on the sea surface roughness and on geometrical conditions. The calmer the sea surface, the more intense will be the reflection from the surface to the sensor on board the satellite. Since a region of calm water may correspond to an area of upwelling, therefore sunglint interpretation can provide information for fishing operations. In 1954-1956 Cox and Munk used aerial photographs and studied sunglint. They correlated the statistical distribution of sea surface slope with wind velocity. The slicks, ripples areas and eddies can be seen in the sunglint areas (Soules 1970). Wald and Monget (1983) worked on different data from different satellites and reported the usefulness of space sunglint contaminated photographs for the determination of wind velocity. They have adopted a method of calculating wind velocity in terms of the recorded intensity. In their method one has to know the intensity values all over the scenes.

3.0 NEED OF AUTOMATIC IDENTIFICATION OF SUNGLINT AREAS

Keeping in view the inconvenience and usefulness of the sunglint and the oceanographers' increasing interest in interpreting and utilizing sunglint-contaminated images, the exploration for petroleum and cleaning up of the environment with the help of sunglint-contaminated space imagery, it is important for the users to know the location of the sunglint area on the scenes under consideration. Taking into account the inconvenience of the sunglint on the one hand and the usefulness on the other hand, we have developed software for the identification of sunglint areas on AVHRR scenes archived

at the Dundee University receiving station. The Dundee archive of AVHRR data contains more than 12,000 scenes from the launch of TIROS-N in 1978 until the present time. This software in fact will eliminate the need for tedious visual inspection to identify all those scenes in which sunglint is possible from the Sun-Earth-satellite geometry and will help in making the interpreter aware of the location of the sunglint area.

4.0 OFF-NADIR POINTS LATITUDE AND LONGITUDE

Let Φ_s and λ_s, respectively, be the latitude and longitude of a subsatellite point along a scan line that makes an angle 'j' equal to the angle of inclination (the angle the satellite track makes with the polar axis). The triangle thus formed by the equatorial meridian, the meridian passing through the point on the scan line and the part of the scan line from the ascending (or descending) node to the point will be a spherical right-angled triangle. The length of the scan line in terms of pixel size and pixel number can be worked out if the pixel dimension within the scan line is known. Let it be P_n where P denotes pixel size and n the number of pixels. Then with the help of spherical trigonometry the longitude, L_o, from the ascending node (subsatellite point) to the meridian that passes through the point of interest is given by

$$\tan(L_o) = \tan(P_n)\cos(j) \tag{1}$$

and the latitude which will be either less or greater than the subsatellite latitude (depending upon which side the off-nadir point is situated relative to the ascending node) can be calculated from the following equation

$$\sin(L_a) = \sin(P_n)\sin(j) \tag{2}$$

where L_a stands for the nadir point latitude. The latitude of a point lying on the left-hand side of the nadir point would be less than the nadir point latitude by an amount given by equation (2). The actual longitude and latitude of an off-nadir point can be obtained respectively as

$$\lambda_o = \lambda_s + L_o \tag{3}$$

$$\Phi_o = \Phi_s - L_a \tag{4}$$

It is interesting that the size variation of the pixels along a scan line from nadir towards off-nadir was calculated by a very simple method. This variation was compared with the variation derived by Hayes and Cracknell (1984) and Singh and Cracknell (1986) and was found to be in good agreement. This variation with the number of pixels from nadir towards off-nadir is shown in figure 1.

5.0 WIND VELOCITY AND SUNGLINT RADIANCE

In order to find the sunglitter radiance we have used an empirical formula (see equation (6)) for the determination of the water-leaving-radiance for the central wavelength 0.9125 μm. The radiance reflected from the surface of the Earth to the sensor is the sum of the water-leaving-radiance, the sky radiance and the sunglitter radiance and can be written symbolically as

$$L_s(\lambda) = L_w(\lambda) + L_{sk}(\lambda) + L_g(\lambda) \tag{5}$$

where $L_s(\lambda)$ is the satellite-measured radiance from the surface of the Earth, $L_{sk}(\lambda)$ is the diffuse sky radiance, $L_g(\lambda)$ is the sunglitter radiance and $L_w(\lambda)$ which represents the water-leaving radiance was calculated from

$$L_w(\lambda) = \frac{\tau_r}{\tau_a} \rho \frac{E_g}{\pi} \tag{6}$$

where τ_r and τ_a respectively represent the Rayleigh and aerosol optical thicknesses, E_g is the global irradiance and ρ the average of surface reflectivities for the zenith angle of the Sun, θ_s, and the zenith
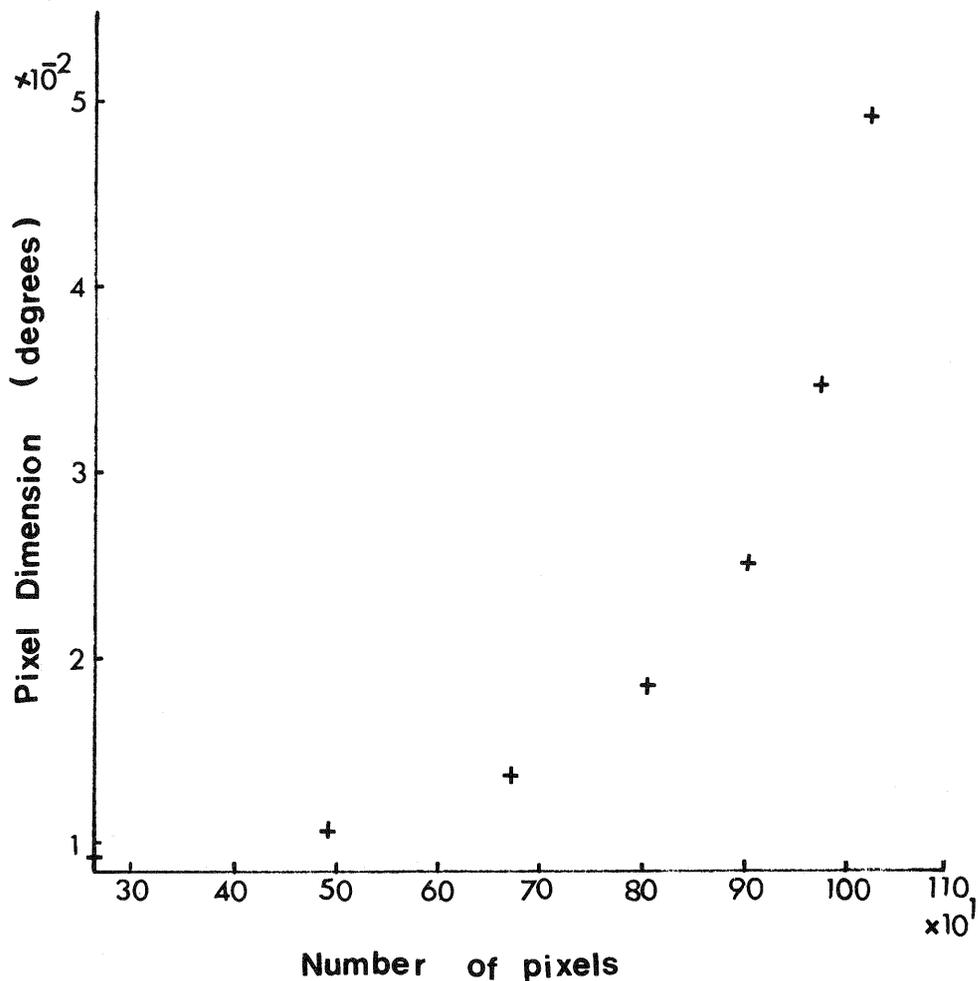
Figure 1: Pixel size versus pixel number along a scan line.

angle of the sensor, θ. Its value is kept constant and is equal to 0.042. $L_s(\lambda)$ was computed from the digital data obtained from the computer-compatible tape. Reference can be made to Singh and Cracknell (1986) for the determination of $L_s(\lambda)$. From $L_s(\lambda)$ and $L_g(\lambda)$ it is now possible to find the mean square slope from the relation

$$\frac{L_g(\lambda)\cos^4\theta_n\cos\theta}{L_s(\lambda)r(\omega)} = P(\theta_n, V) \tag{7}$$

where $r(\omega)$ is the Fresnel reflectity for the incidence angle ω, $P(\theta_n, V) = \frac{1}{\sigma^2}\exp(-\frac{\tan^2\theta_n}{\sigma^2})$ and the mean square slope σ^2 as given by Cox and Munk (1954, 1956) is related to wind speed V in metres per second as

$$\sigma^2 = 0.003 + 0.00512\ V \tag{8}$$

In equation (7) the values of σ^2 were computed by iteration.

6.0 RESULTS

The program was run for calculating the location of the sunglint area in 31 sets of NOAA-7 data from summer 1982 and summer 1983. The latitudes and longitudes were compared with the visual sunglint areas in the corresponding quicklook images. Three of the scenes in which the arrows show the calculated sunglint area are shown in figures 2, 3 and 4. The program has been run for the NOAA-7 orbits and the latitude for the run was limited up to 45 degrees north. It would work for the
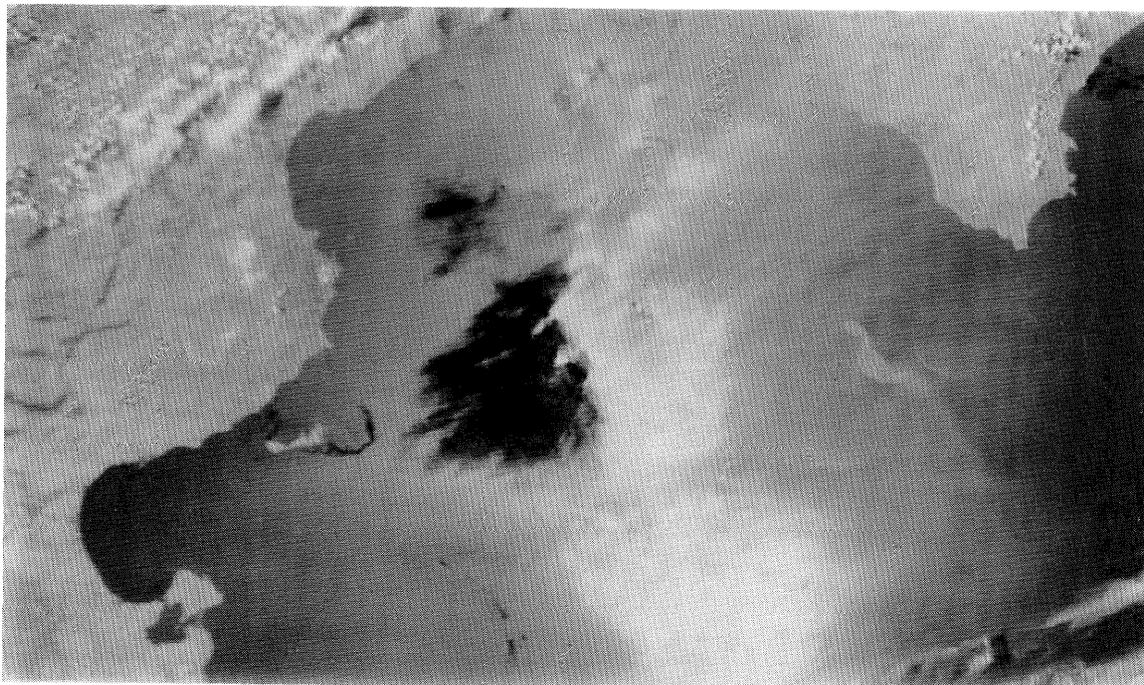
Figure 2: NOAA-7 scene showing sunglint area, date 23 May 1982, orbit no. 4715.
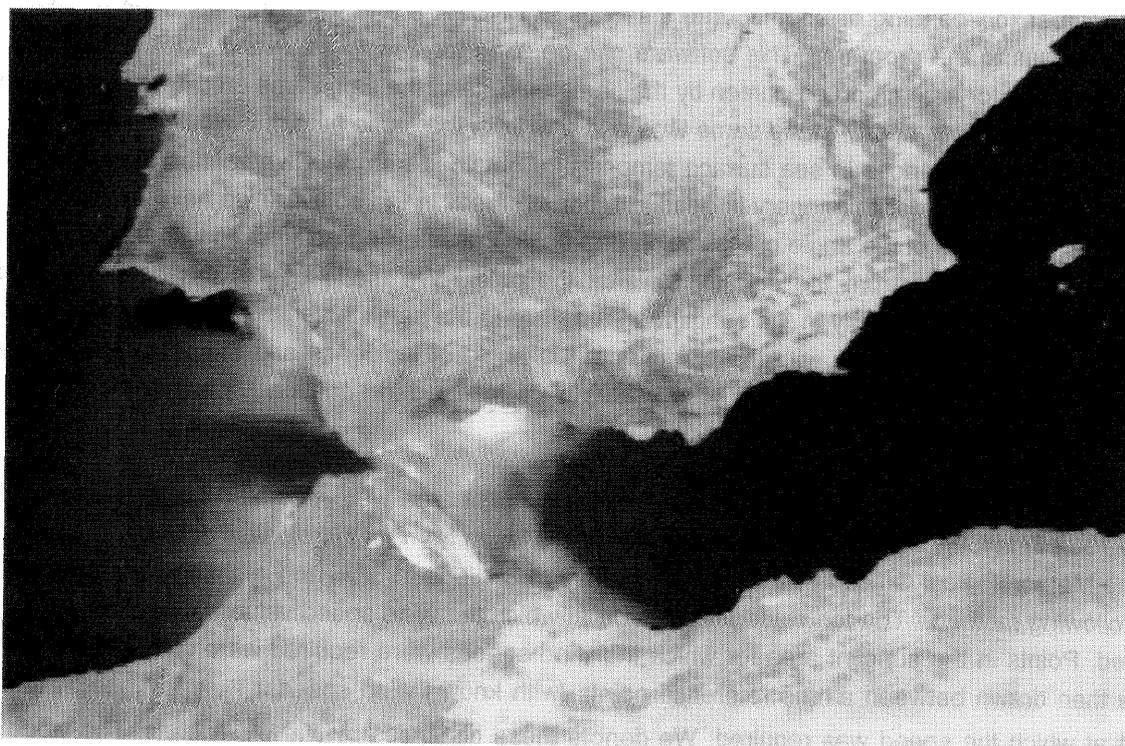

Figure 3: NOAA-7 scene showing sunglint area, date 28 June 1982, orbit no. 5224.
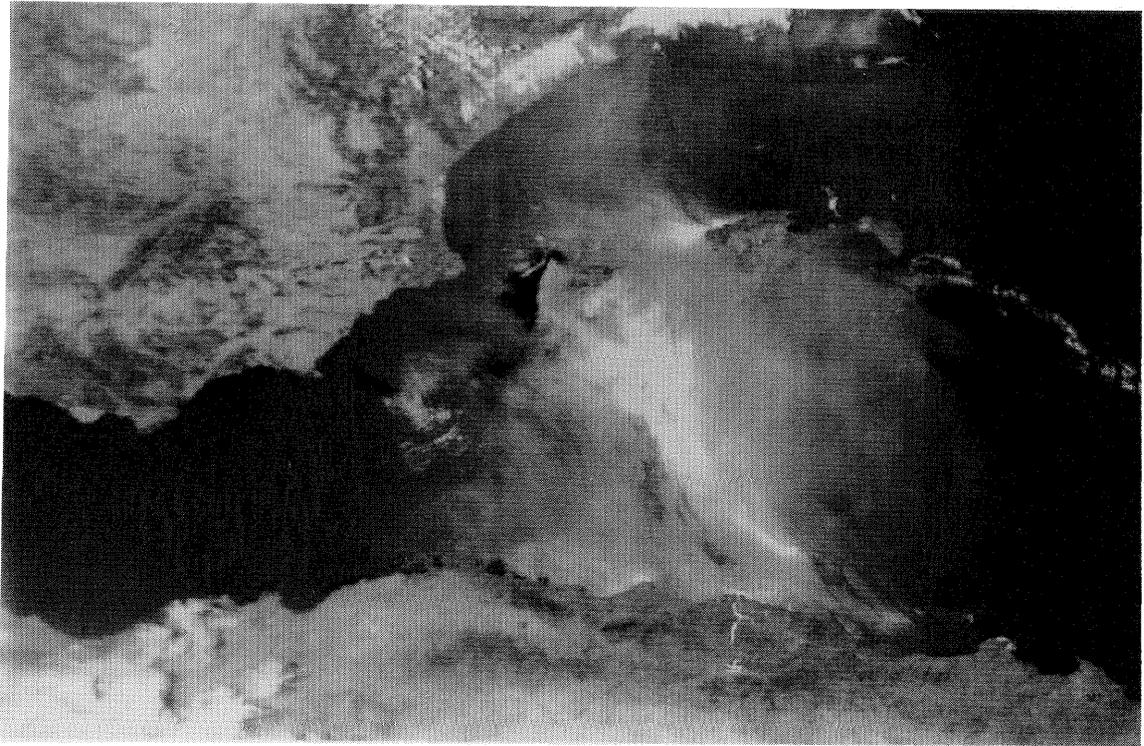
Figure 4: NOAA-7 scene showing sunglint area, date 1 July 1983, orbit no. 10420.

even number (descending or southbound) satellites like NOAA-8 and for higher latitudes by making slight changes to the program. This software can be used for finding solar and satellite zenith and azimuth angles for a common area seen by the same satellite at the same time on different days or by two different satellites nearly at the same time and day from the same height. It would make the user able to find the differences in sea surface temperature obtained from the two scenes. From this one can also find which satellite imagery is good in a certain area. In the software we have not taken into account the increase of the angle of inclination (the angle the satellite track makes with the polar axis) as the satellite moves from the equator towards the pole. We made use of this software in the determination of wind velocity in the sunglint area by taking the satellite zenith angle, the angle θ_n the normal to the surface makes with the plumb line, the angle of incidence and the solar zenith angle from the results obtainable from it. These values were inserted in equation (7) and finally the wind speed was determined.

The values of windspeed for 34 points within the sunglint area were weighted for the scene of 15 June 1982 in favour of those limited points which were taken from meteorological data kindly provided by the Meteorological Office at Bracknell for 13 May to 27 June 1982. The weighting was done using the following method. The longitude and latitude at which the wind speed values were availabe were plotted. Points in the sunglint area for which the wind speeds were required were also plotted. Lines were then drawn between all the reference points (with known wind speeds) V_1, V_2, V_3,...etc., and a point at which the speed was required. We denote these distances by R_1, R_2, R_3,...etc. The value of wind speed at this required point was then calculated by using the expression

122

$$V(mean\ weighted) = \frac{\sum_i V_i (1/R_i)^2}{\sum_i (1/R_i)^2}$$

(9)

This process was then repeated for the remaining points. Table 1 shows the weighted and computed wind speeds and the differences between them.

Table 1: Wind speeds

No.	Weighted (m/s)	Computed (m/s)	Difference (m/s)	No.	Weighted (m/s)	Computed (m/s)	Difference (m/s)
1	4.7	4.0	0.7	18	5.0	4.7	0.3
2	4.3	4.1	0.7	19	4.7	4.9	-0.2
3	4.9	4.1	0.8	20	4.6	5.4	-0.8
4	4.9	4.1	0.8	21	4.8	5.4	-0.6
5	4.9	4.2	0.7	22	5.1	5.7	-0.6
6	5.0	4.2	0.8	23	4.6	3.7	0.9
7	5.0	4.8	0.2	24	5.0	4.4	0.6
8	5.0	4.4	0.6	25	5.0	4.7	0.3
9	5.0	4.5	0.5	26	4.9	5.2	-0.3
10	5.0	4.8	0.2	27	4.9	4.4	0.5
11	5.0	5.0	0.0	28	5.1	4.3	0.8
12	4.8	5.2	-0.4	29	4.9	5.3	-0.4
13	4.6	4.6	0.0	30	4.8	5.2	-0.4
14	4.2	4.9	-0.7	31	6.2	5.2	1.0
15	4.2	4.9	-0.7	32	5.0	4.4	0.6
16	4.7	4.9	-0.2	33	5.5	4.5	1.0
17	4.7	4.7	0.0	34	5.0	4.8	0.2

7.0 CONCLUSIONS

The software developed for the sunglint identification in AVHRR data is simple and can save time for AVHRR data users who are either looking for or trying to avoid the sunglint area on the data. The results of the software can be used in evaluating wind speeds within the sunglint area. The wind speeds calculated for 34 scattered points in the sunglint area in a scene of 15 June 1982 are quite encouraging. The standard deviation obtained from the data is about 0.5 m/s. Further work will be carried out utilizing more scenes for which we have corresponding in situ data.

Acknowledgement:

References:

Burstein, R.L. (1982): Sea surface temperature estimation using NOAA-6 satellite Advanced Very High Resolution Radiometer. J. Geophys. Res., 87, 9455-9465.

Cox, C. and Munk, W. (1954): Statistics of the sea surface derived from sunglitter. Journal of Marine Research, 13, 198-227.

Cox,C. and Munk, W. (1956): Slopes of the sea surface deduced from photographs of sun glitter. Bulletin of the Scripps Institute of Oceanography, 6, 401-488.

Hayes, L. and Cracknell, A.P. (1984): A comparison of TIROS-N series satellite data over Scotland. Proc: Integrated approach in Remote Sensing Guildford U.K. April 8-11, (Paris ESA SP-214), 63-74.

Hoge, F.E. and Swift, R.N. (1987): Ocean colour spectral variability studies using solar induced fluorescence. Applied Optics, 26, 18-20.

Singh, S.M. and Cracknell, A.P. (1986): The Estimation of atmospheric effects for SPOT using

AVHRR channel-1 data. Int. J. Remote Sensing, 7, 361-377.

Soules, S.D. (1970): Sunglitter viewed from space. Deep Sea Research, 17, 191-195.

Takashima, T. and Takayama, Y. (1981): Estimation of sea surface temperature from remote sensing in the 3.7 µm window region. Journal of Meteorological Society, Japan, 59, 876-890.

Wald, L. and Monget, J.M. (1983): Sea surface winds from sun glitter observations. J. Geophy. Res., 88, 2547-2555.